Halogen substituted bithiophene-based polycatenars with tunable fluorescence

Mohamed Alaasar,[a,b*] Yu Cao,[c,d] Thorben Neumann,[e] Tianyi Tan,[c] Feng Liu,[c] Michael Giese,[e*]

[a]Institute of Chemistry, Martin Luther University Halle-Wittenberg, 06120 Halle, Germany
[b]Department of Chemistry, Faculty of Science, Cairo University, 12613 Giza, Egypt
[c]Shaanxi International Research Center for Soft Matter, State Key Laboratory for Mechanical Behavior of Materials, Xi'an Jiaotong University, Xi'an 710049, P. R. China
[d]Guangdong Provincial Key Laboratory of Functional and Intelligent Hybrid Materials and Devices, Guangzhou 510641, China
[e]Organic Chemistry, University of Duisburg Essen, Universitätsstraße 7, Essen 45117, Germany

Contents

1. Synthesis

Synthesis of the target polycatenars AXY.

General procedure. A solution of 4-*n*-hexyloxysubstituted benzoic acid **1XY** [1] (1 equivalent) in 2 mL $SOCl_2$ and two drops of *N,N*-dimethylformamide (DMF) was refluxed for 1 hour. The excess thionyl chloride was removed under reduced pressure. The phenol **2** [2] (1 equivalent) previously dissolved in 25 mL of dichloromethane (DCM) together with triethylamine (1.2 equivalent) and a catalytic amount of pyridine were added to the acid chloride. The mixture was refluxed for 6 hours and monitored by TLC. Extraction was performed with DCM and the organic layer was washed with water, dried over anhydrous Na_2SO_4 followed by removal of the solvent under reduced pressure. The obtained crude material was purified using column chromatography using $CHCl_3$/*n*-Hexane 4:1 followed by a final step of recrystallization from ethanol/chloroform mixture (2:1) to afford the desired materials as yellow crystals.

4-(5'-(4-((3,5-bis(heptyloxy)benzoyl)oxy)phenyl)-[2,2'-bithiophen]-5-yl)phenyl-3-fluoro-4-(hexyloxy)benzoate, AFH

Yellow crystals. Yield 73.75%; ^{1}H NMR (400 MHz, $CDCl_3$) δ 7.97 (dt, *J* = 8.4, 1.6 Hz, 1H), 7.91 (dd, *J* = 11.5, 2.1 Hz, 1H), 7.65 (d, *J* = 8.4 Hz, 4H, Ar-H), 7.32 (d, *J* = 2.3 Hz, 2H, Ar-H), 7.29 – 7.14 (m, 8H, Ar-H overlapped with $CHCl_3$ signal), 7.04 (t, *J* = 8.3 Hz, 1H, Ar-H), 6.72 (t, *J* = 2.3 Hz, 1H, Ar-H), 4.13 (t, *J* = 6.6 Hz, 2H, Ar-O$\underline{CH_2}$-), 4.01 (t, *J* = 6.5 Hz, 4H, Ar-O$\underline{CH_2}$-), 1.93 – 1.74 (m, 6H, Ar-OCH$_2\underline{CH_2}$-), 1.60 – 1.23 (m, 22H, 2 x 11 CH_2), 0.99 – 0.82 (m, 9H, 3 x CH_3). ^{13}C NMR (126 MHz, $CDCl_3$) δ 165.16 (C=O), 164.16 (d, $^4J_{C,F}$ = 2.5 Hz, C=O), 160.49 (2C, C_{ar} -O), 153.07, 152.24, 152.16, 151.10, 150.62, 150.51 (4C, including 2d, C_{ar}-O, C_{ar}-F), 142.45, 142.41, 136.98, 136.96, 132.07, 132.04, 131.19, 127.58, 127.55 (C_{ar}),[a] 126.87 (4C, C_{ar} -H), 124.76 (2C, C_{ar}) 124.23, 124.21 (C_{ar}),[a] 122.41, 122.38 (2x2C, C_{ar} -H), 121.89, 121.84, 118.07, 117.91, 113.63, 113.62 (C_{ar}),[a] 108.40 (2C, C_{ar}-H), 107.40 (C_{ar}-H), 69.64 (OCH_2), 68.61 (2C, OCH_2), 31.93 (2C, CH_2), 31.65 (CH_2), 29.35 (2C, CH_2), 29.19 (2C, CH_2), 29.12 (CH_2), 26.14 (2C, CH_2), 25.70 (CH_2), 22.76 (2C, CH_2), 22.71 (CH_2), 14.23 (2C, CH_3), 14.15 (CH_3);[a] among the C_{ar} signals there are 4d due to the coupling with F; C_{ar} involves quaternary carbons as well as C_{ar}-H. ^{19}F NMR (470 MHz, $CDCl_3$) δ -133.58 (dd, *J* = 11.4, 8.0 Hz). EA: calculated for $C_{54}H_{61}FO_7S_2$: C 71.65%, H 6.79%; found: C 71.58%, H 6.77%.

4-(5'-(4-((3,5-bis(heptyloxy)benzoyl)oxy)phenyl)-[2,2'-bithiophen]-5-yl)phenyl-2-fluoro-4-(hexyloxy)benzoate, AHF

Yellow crystals. Yield 74.98%; ^{1}H NMR (400 MHz, $CDCl_3$) δ 8.05 (t, *J* = 8.6 Hz, 1H, Ar-H), 7.73 – 7.57 (m, 4H, Ar-H), 7.36 – 7.13 (m, 10H, Ar-H overlapped with $CHCl_3$ signal), 6.78 (dd, *J* = 8.9, 2.4 Hz, 1H, Ar-H), 6.75 – 6.65 (m, 2H, Ar-H), 4.10 – 3.95 (m, 6H, Ar-O$\underline{CH_2}$-), 1.88 – 1.73 (m, 6H, Ar-OCH$_2\underline{CH_2}$-), 1.64 – 1.21 (m, 22H, 2 x 11 CH_2), 1.00 – 0.82 (m, 9H, 3 x 3 CH_3). ^{13}C NMR (126 MHz, $CDCl_3$) δ 165.16 (C=O), 162.63 (d, $^{4}J_{C,F}$ = 4.6 Hz, C=O), 160.50, (2 x OAr), 152.91, 152.25, 151.68, 151.12, 150.61, 150.42, (4C, including 2d, C_{ar}-O, C_{ar}-F), 142.52, 142.42, 137.00, 136.92, 134.01, 133.99, 132.06, 131.98, 131.20 (C_{ar}),[a] 126.87, 126.82 (2 x 2C, C_{ar-H}), 124.76, 124.75 (C, C_{ar}), 124.21, 124.19 (C_{ar}),[a] 122.49, 122.41 (2 x 2C, C_{ar-H}), 110.06, 110.04 (C_{ar}),[a] 108.41 (2C, C_{ar-H}), 107.41, 103.15, 102.95 (C, C_{ar-H}), 69.02 (OCH_2), 68.61 (2C, OCH_2), 31.93 (2C, CH_2), 31.65 (CH_2), 29.35 (2C, CH_2), 29.19 (2C, CH_2), 29.06 (CH_2), 26.14 (2C, CH_2), 25.75 (CH_2), 22.76 (2C, CH_2), 22.72 (CH_2), 14.23 (2C, CH_3), 14.15 (CH_3);[a] among the C_{ar} signals there are 4d due to the coupling with F; C_{ar} involves quaternary carbons as well as C_{ar}-H. ^{19}F NMR (470 MHz, $CDCl_3$) δ -104.55 (dd, *J* = 12.6, 8.5 Hz). EA: calculated for $C_{54}H_{61}FO_7S_2$: C 71.65%, H 6.79%; found: C 71.60%, H 6.75%.

4-(5'-(4-((3,5-bis(heptyloxy)benzoyl)oxy)phenyl)-[2,2'-bithiophen]-5-yl)phenyl-2,3-difluoro-4-(hexyloxy)benzoate, AFF

Yellow crystals. Yield 73.62%; ^{1}H NMR (500 MHz, $CDCl_3$) δ 7.86 (ddd, *J* = 9.7, 7.6, 2.2 Hz, 1H, Ar-H), 7.69 – 7.63 (m, 4H, Ar-H), 7.33 (d, *J* = 2.3 Hz, 2H, Ar-H), 7.29 – 7.21 (m, 7H, Ar-H overlapped with $CHCl_3$ signal), 7.19 (d, *J* = 3.7 Hz, 2H, Ar-H), 6.87 – 6.80 (m, 1H, Ar-H), 6.72 (t, *J* = 2.3 Hz, 1H, Ar-H), 4.15 (t, *J* = 6.6 Hz, 2H, Ar-O$\underline{CH_2}$-), 4.02 (t, *J* = 6.5 Hz, 4H, Ar-OCH$_2\underline{CH_2}$-), 1.93 – 1.75 (m, 6H), 1.59 – 1.27 (m, 22H, 2 x 11 CH_2), 0.98 – 0.85 (m, 9H, 3 x 3 CH_3). ^{13}C NMR (126 MHz, $CDCl_3$) δ 165.16 (C=O), 162.16 -162.10 (m, C=O), 160.50 (2C, C_{ar} -O), 153.12, 153.03, 151.03, 150.94, 150.62, 150.21 (4C, including 2d, C_{ar}-O, C_{ar}-F) 142.46, 142.37, 137.02, 137.95, 132.19, 132.05, 131.20, 127.21, 127.18 (C_{ar}),[a] 126.87, 126.85 (2x2C, C_{ar-H}), 124.78, 124.76 (C, C_{ar}), 124.27 (2C, C_{ar}), 124.22 (C_{ar}),[a] 122.41, 122.37 (2x2C, C_{ar-H}), 111.40, 111.34, 108.64, 108.62 (C_{ar}),[a] 108.41 (2C, C_{ar-H}), 107.41 (C_{ar}), 70.16 (OCH_2), 68.61 (2C, OCH_2), 31.93 (2C, CH_2), 31.61 (CH_2), 29.35 (2C, CH_2), 29.19 (2C, CH_2), 29.06 (CH_2), 26.14 (2C, CH_2), 25.63 (CH_2), 22.76 (2C, CH_2), 22.69 (CH_2), 14.23 (2C, CH_3), 14.19 (CH_3);[a] among the C_{ar} signals there are 4d due to the coupling with F; C_{ar} involves quaternary carbons as well as C_{ar}-H. ^{19}F NMR (470 MHz, $CDCl_3$) δ -132.04 – -132.14 (m), -157.94 (ddd,

J = 19.6, 7.1, 2.4 Hz). EA: calculated for $C_{54}H_{60}F_2O_7S_2$: C 70.25%, H 6.55%; found: C 70.19%, H 6.54%.

4-(5'-(4-((3,5-bis(heptyloxy)benzoyl)oxy)phenyl)-[2,2'-bithiophen]-5-yl)phenyl-2-chloro-4-(hexyloxy)benzoate, AHCl

Yellow crystals. Yield 73.50%; ^{1}H NMR (500 MHz, $CDCl_3$) δ 8.11 (d, *J* = 8.8 Hz, 1H, Ar-H), 7.69 – 7.63 (m, 4H, Ar-H), 7.33 (d, *J* = 2.3 Hz, 2H, Ar-H), 7.30 – 7.21 (m, 6H, Ar-H overlapped with $CHCl_3$ signal), 7.19 (d, *J* = 3.8 Hz, 2H, Ar-H), 7.04 (d, *J* = 2.5 Hz, 1H, Ar-H), 6.90 (dd, *J* = 8.9, 2.5 Hz, 1H, Ar-H), 6.72 (t, *J* = 2.3 Hz, 1H, Ar-H), 4.09 – 3.96 (m, 6H, Ar-O$\underline{CH_2}$-), 1.86 – 1.75 (m, 6H, Ar-OCH$_2\underline{CH_2}$-), 1.58 – 1.27 (m, 22H, 2 x 11 CH_2), 0.98 – 0.86 (m, 9H, 3 x 3 CH_3). ^{13}C NMR (126 MHz, $CDCl_3$) δ 165.16, 163.49 (C=O), 162.99 (C, C_{ar}-O), 160.50 (2C, C_{ar}-O), 150.61, 150.45, 142.48, 142.43, 136.98, 136.96, 134.17, 132.04, 131.20 (C_{ar}),[a] 126.87, 126.84 (2x2C, C_{ar-H}), 124.76 (2x2C, C_{ar}),[a] 124.21 (2x2C, C_{ar}),[a] 122.46, 122.41 (2x2C, C_{ar-H}), 120.34, 117.39, 113.34 (C_{ar}),[a] 108.40 (2C, C_{ar-H}), 107.41(C_{ar}),[a] 68.89 (OCH_2), 68.61 (2C, OCH_2), 31.93 (2C, CH_2), 31.65, 29.35 (2C, CH_2), 29.19 (2C, CH_2), 29.09 (CH_2), 26.14 (2C, CH_2), 25.74 (CH_2), 22.76 (2C, CH_2), 22.72 (CH_2), 14.23 (2C, CH_3), 14.16 (CH_3). [a]C_{ar} involves quaternary carbons as well as C_{ar}-H. EA: calculated for $C_{54}H_{61}ClO_7S_2$: C 70.37%, H 6.67%; found: C 70.29%, H 6.61%.

4-(5'-(4-((3,5-bis(heptyloxy)benzoyl)oxy)phenyl)-[2,2'-bithiophen]-5-yl)phenyl-2-bromo-4-(hexyloxy)benzoate, AHBr

Yellow crystals. Yield 72.99%; ^{1}H NMR (400 MHz, $CDCl_3$) δ 8.11 (d, *J* = 8.8 Hz, 1H, Ar-H), 7.70 – 7.63 (m, 4H, Ar-H), 7.33 (d, *J* = 2.3 Hz, 2H, Ar-H), 7.30 – 7.21 (m, 6H, Ar-H overlapped with $CHCl_3$ signal), 7.19 (d, *J* = 3.8 Hz, 2H, Ar-H), 7.04 (d, *J* = 2.5 Hz, 1H, Ar-H), 6.90 (dd, *J* = 8.9, 2.5 Hz, 1H, Ar-H), 6.72 (t, *J* = 2.3 Hz, 1H, Ar-H), 4.15 – 3.92 (m, 6H, Ar-O$\underline{CH_2}$-), 1.94 – 1.68 (m, 6H, Ar-OCH$_2\underline{CH_2}$-), 1.66 – 1.17 (m, 22H, 2 x 11 CH_2), 1.01 – 0.81 (m, 9H, 3 x 3 CH_3). ^{13}C NMR (101 MHz, $CDCl_3$) δ 165.16, 163.84 (C=O), 162.76 (C, C_{ar}-O), 160.49 (2C, C_{ar}-O), 150.61, 150.45, 142.46, 142.43, 136.97, 134.09, 132.06, 131.20 (C_{ar}),[a] 126.86, 126.85 (2x2C, C_{ar-H}), 124.76 (2C, C_{ar}),[a] 124.68 (C, C_{ar}),[a] 124.22 (2C, C_{ar}),[a] 122.44, 122.41 (2x2C, C_{ar-H}), 122.11 (C_{ar}),[a] 120.88 (2C, C_{ar}),[a] 113.77 (C_{ar}),[a] 108.40 (2C, C_{ar-H}), 107.40 (C_{ar}),[a] 68.89 (OCH_2), 68.61 (2C, OCH_2), 31.93 (2C, CH_2), 31.65, 29.35 (2C, CH_2), 29.19 (2C, CH_2), 29.10 (CH_2), 26.14 (2C, CH_2), 25.74 (CH_2), 22.76 (2C, CH_2), 22.72 (CH_2), 14.23 (2C, CH_3), 14.16 (CH_3).[a] C_{ar} involves quaternary carbons as well as C_{ar}-H. EA: calculated for $C_{54}H_{61}BrO_7S_2$: C 67.13%, H 6.36%; found: C 67.08%, H 6.30%.

2. NMR Spectra

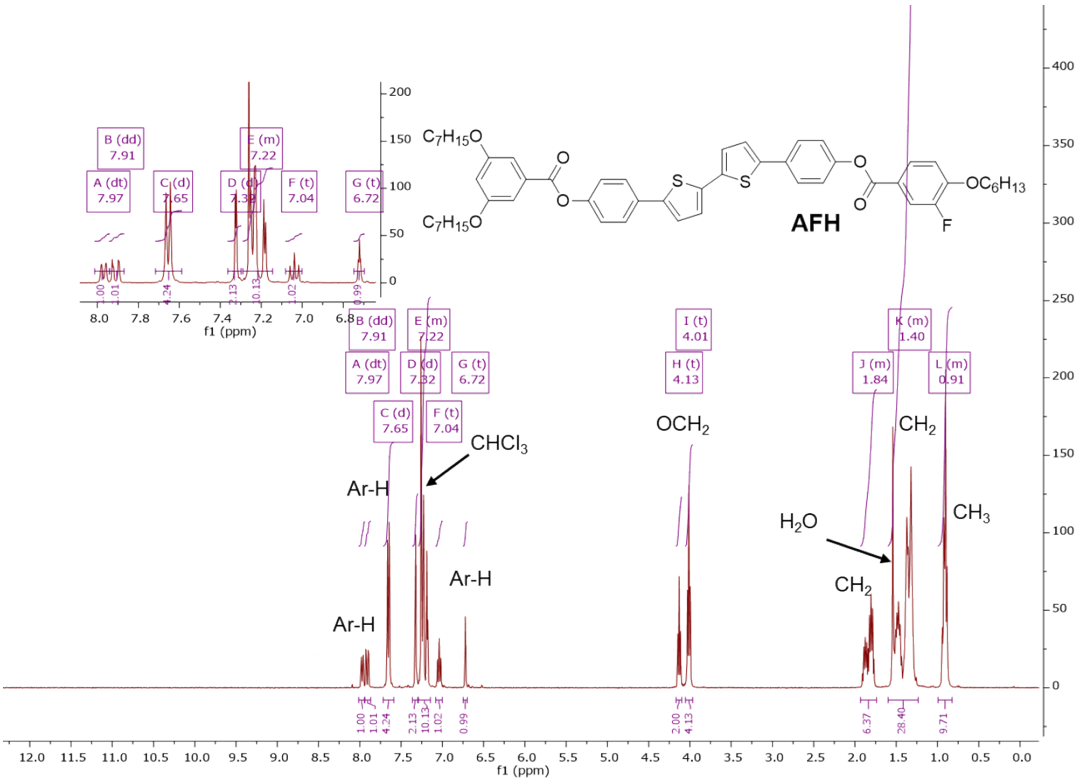

Figure S1. ^{1}H-NMR Spectrum of **AFH** in $CDCl_3$.

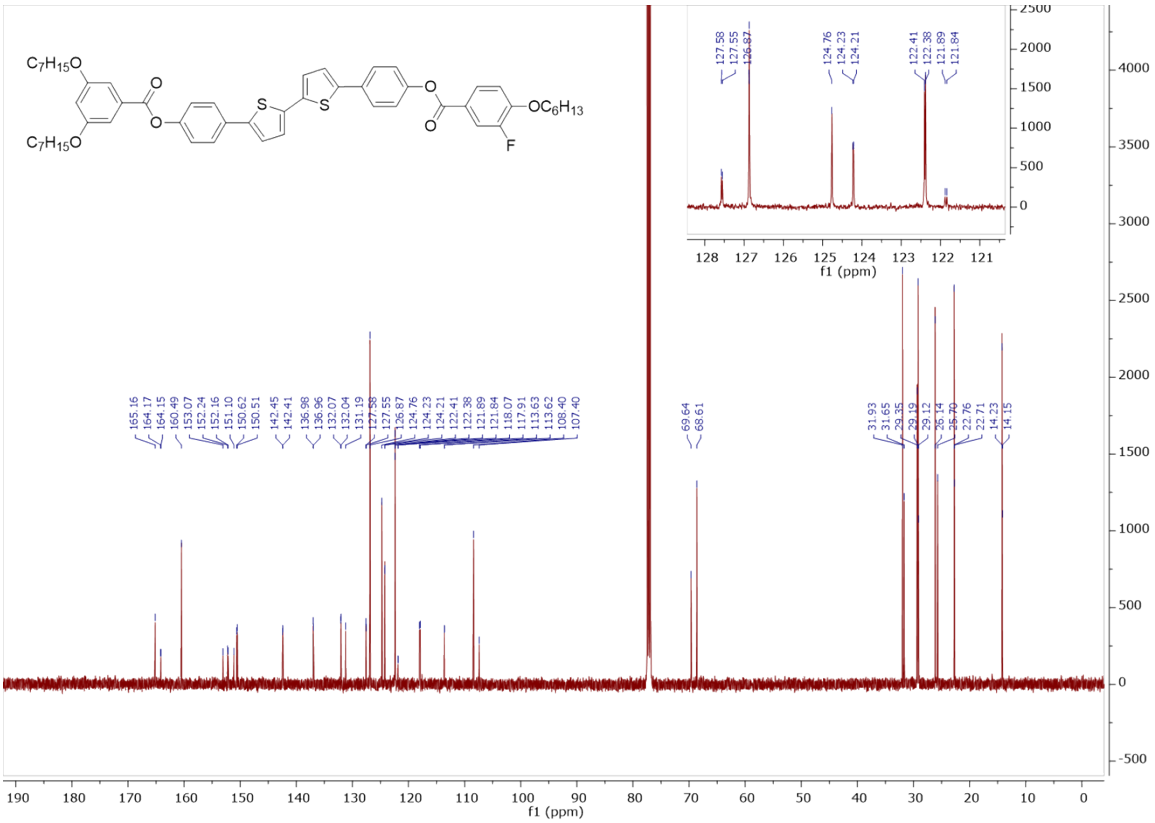

Figure S2. ^{13}C-NMR Spectrum of **AFH** in $CDCl_3$.

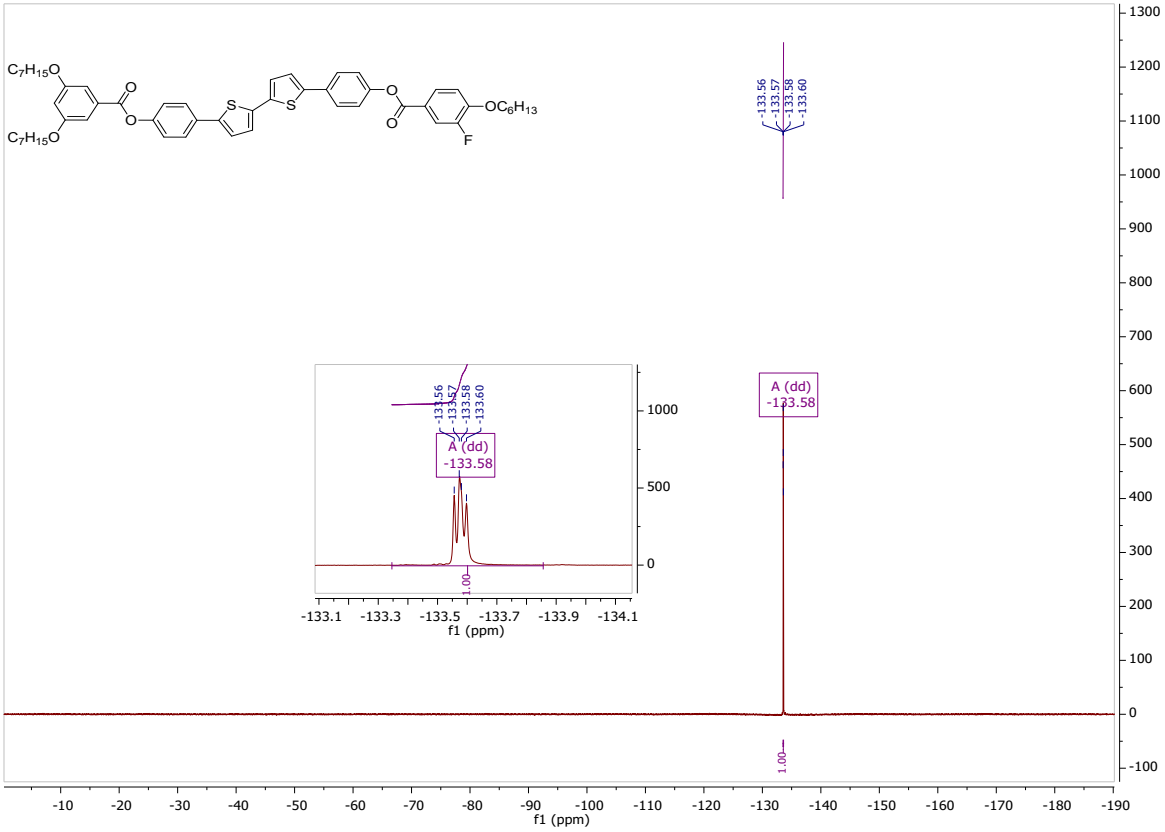

Figure S3. ^{19}F-NMR Spectrum of **AFH** in $CDCl_3$.

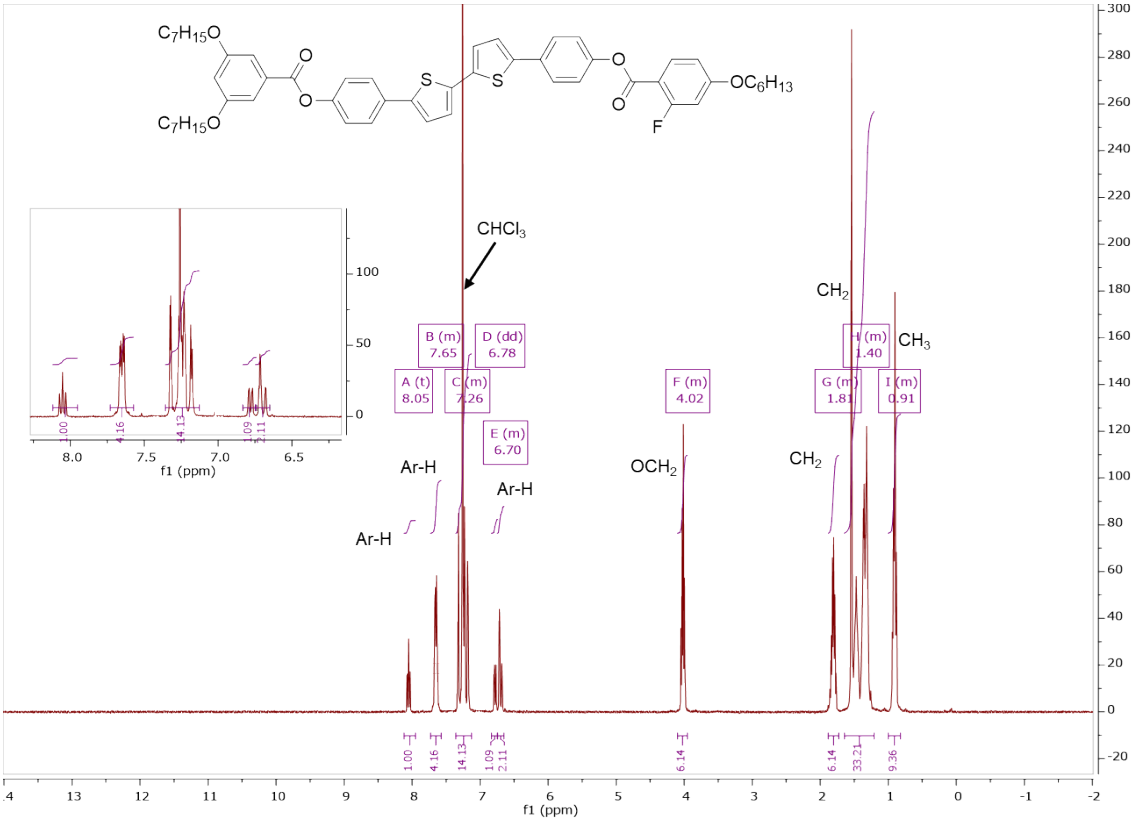

Figure S4. ^{1}H-NMR Spectrum of **AHF** in $CDCl_3$.

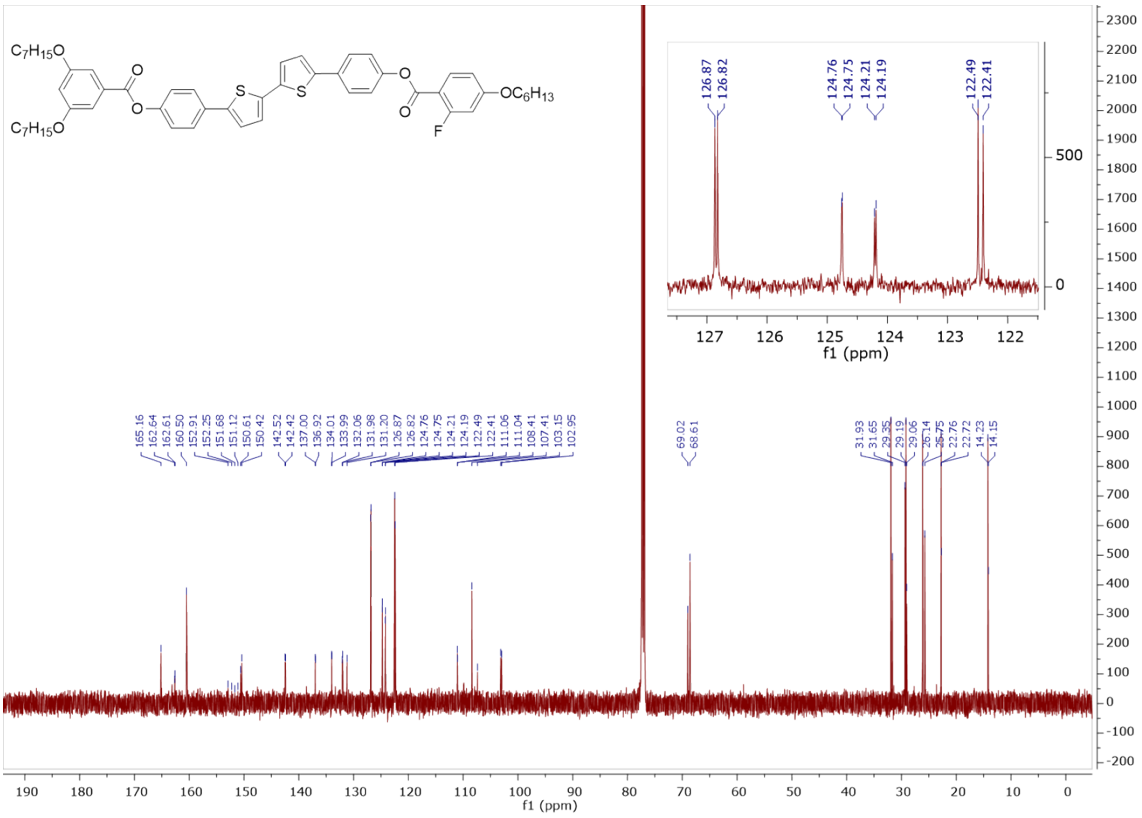

Figure S5. ^{13}C-NMR Spectrum of **AHF** in $CDCl_3$.

Figure S6. ^{19}F-NMR Spectrum of **AHF** in $CDCl_3$.

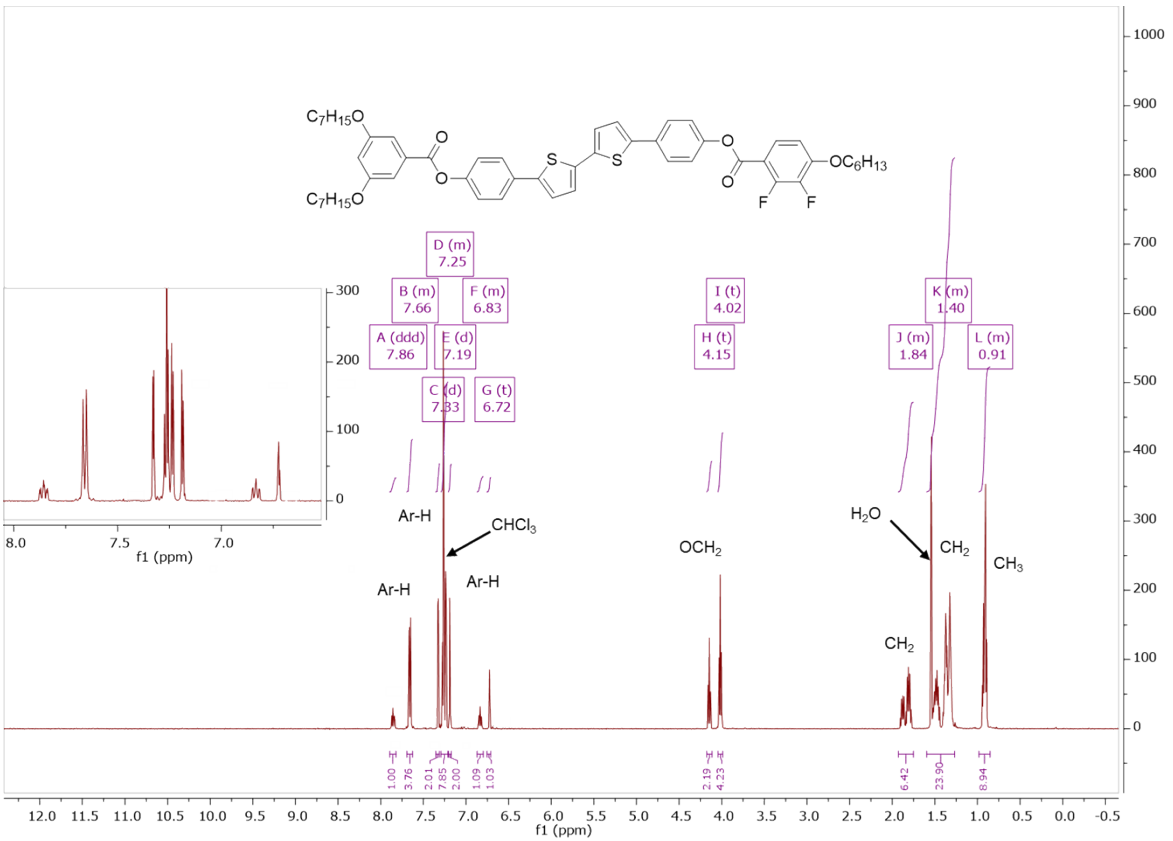

Figure S7. ^{1}H-NMR Spectrum of **AFF** in $CDCl_3$.

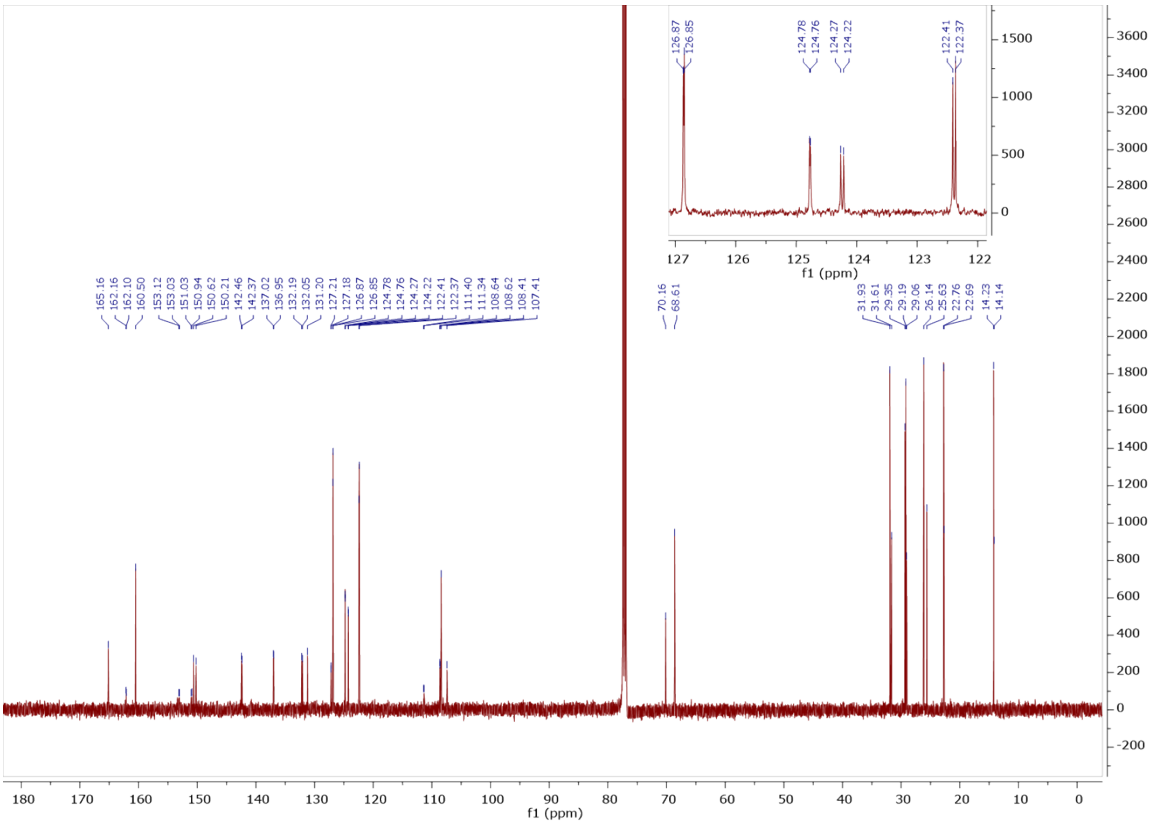

Figure S8. ^{13}C-NMR Spectrum of **AFF** in $CDCl_3$.

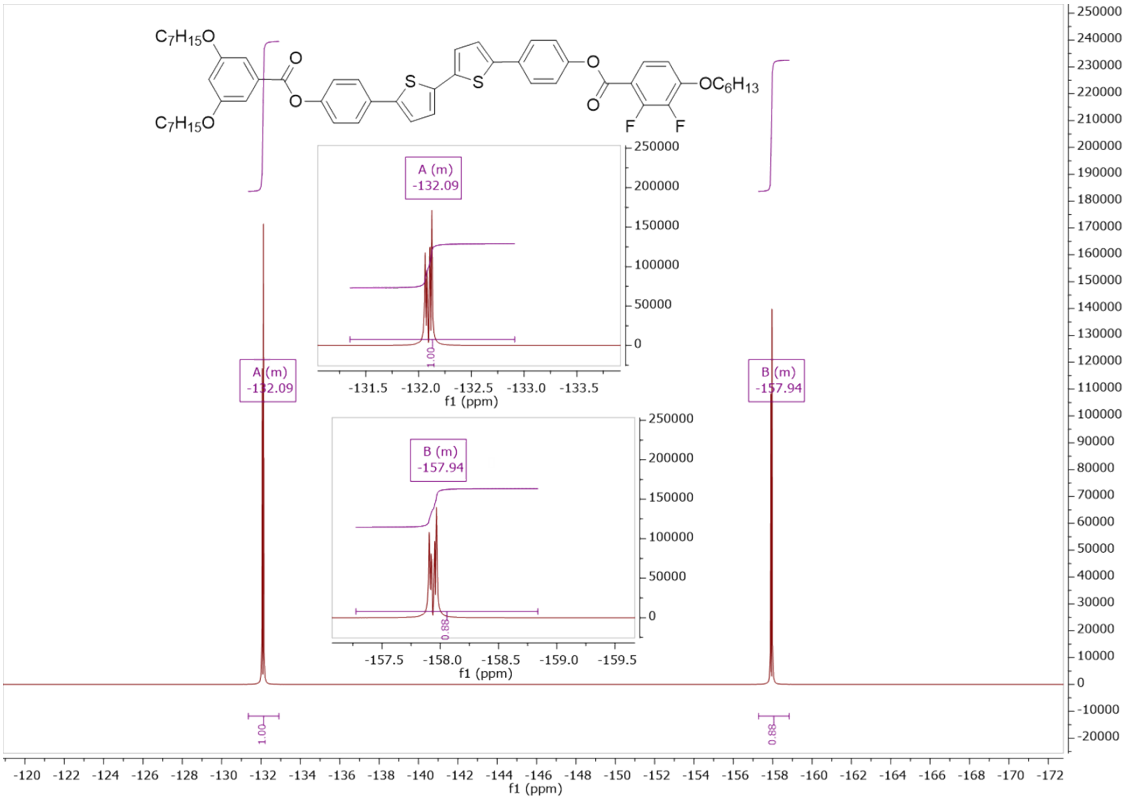

Figure S9. ^{19}F-NMR Spectrum of **AFF** in $CDCl_3$.

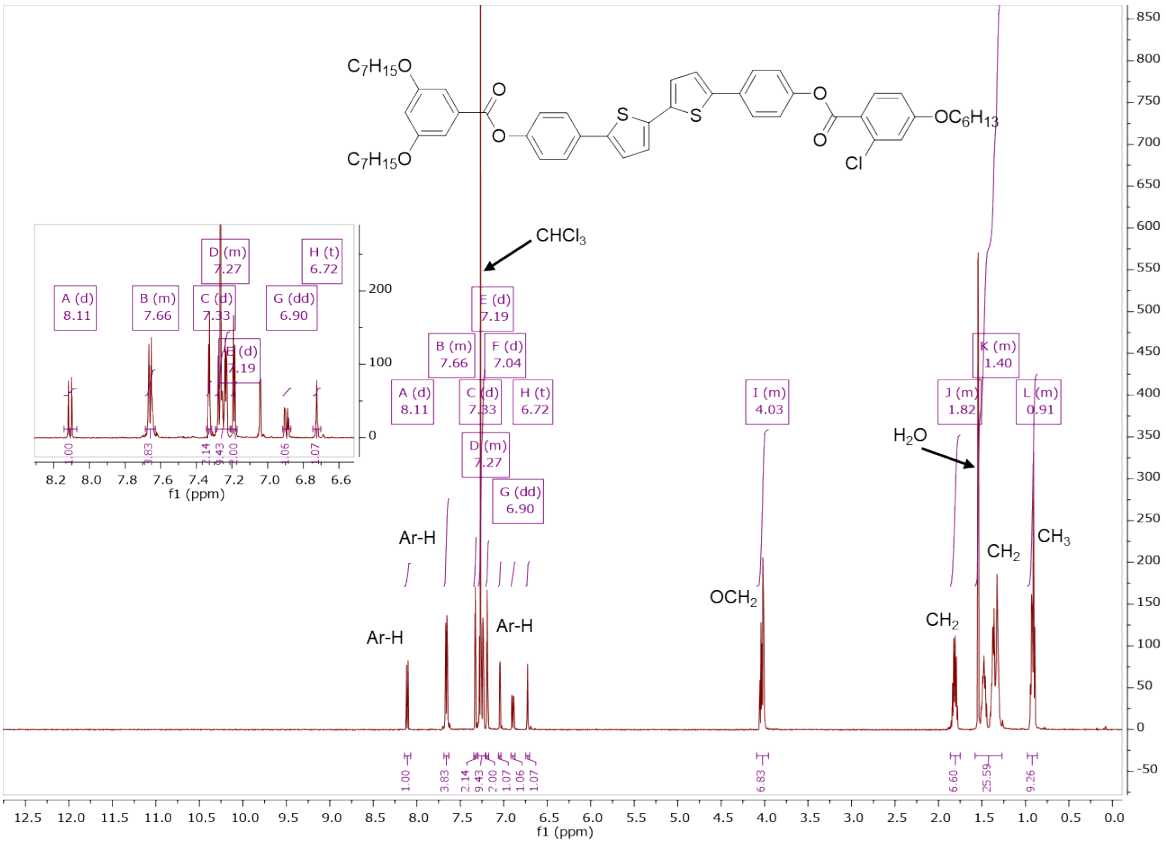

Figure S10. ^{1}H-NMR Spectrum of **AHCl** in $CDCl_3$.

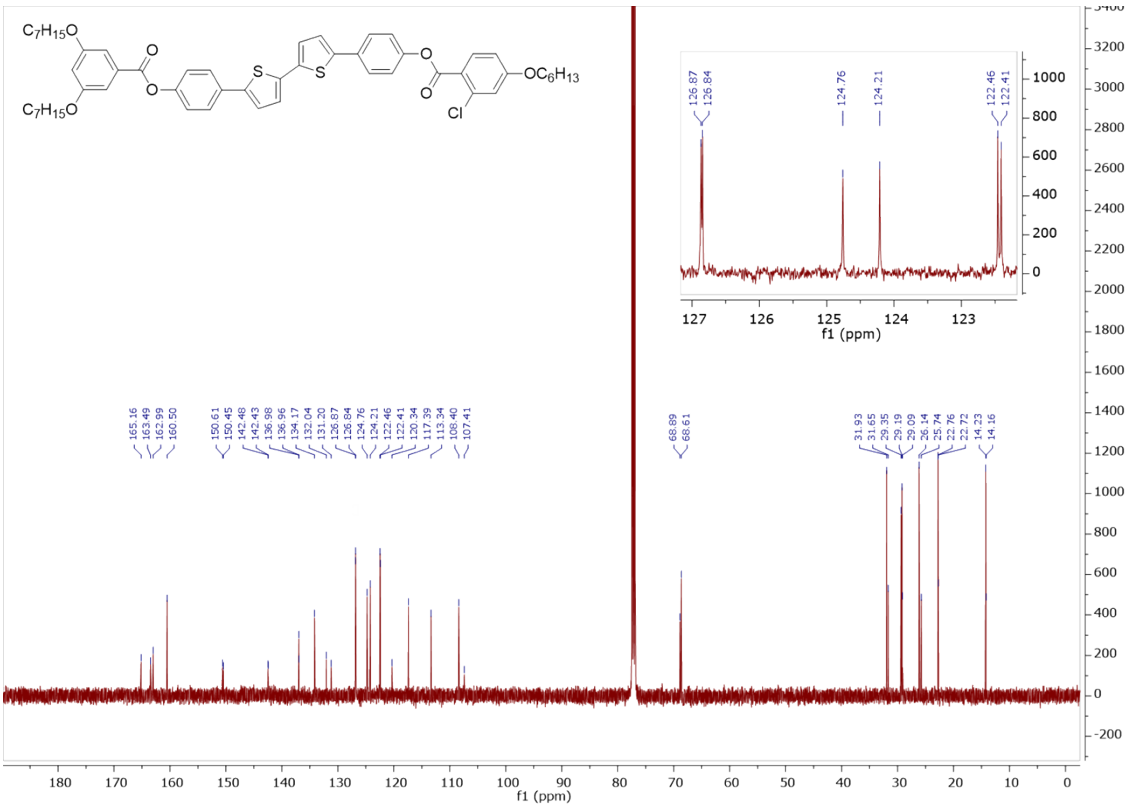

Figure S11. ^{13}C-NMR Spectrum of **AHCl** in $CDCl_3$.

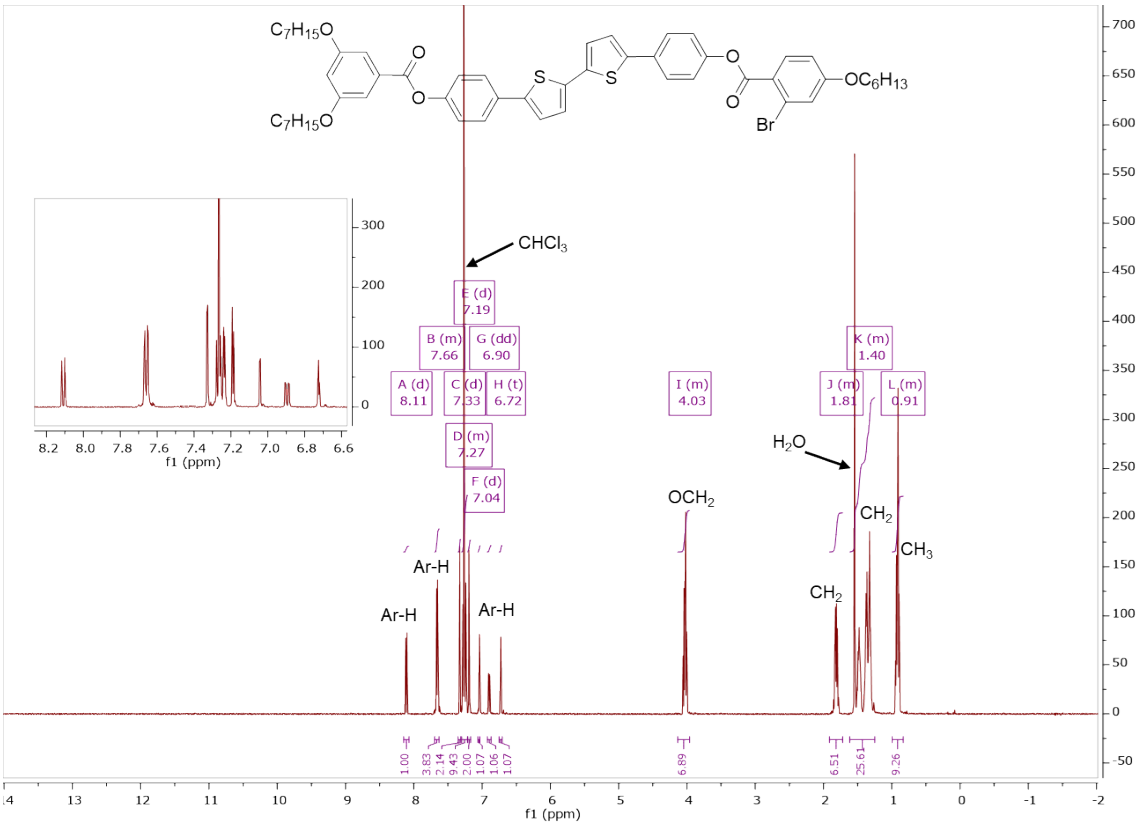

Figure S12. ^{1}H-NMR Spectrum of **AHBr** in $CDCl_3$.

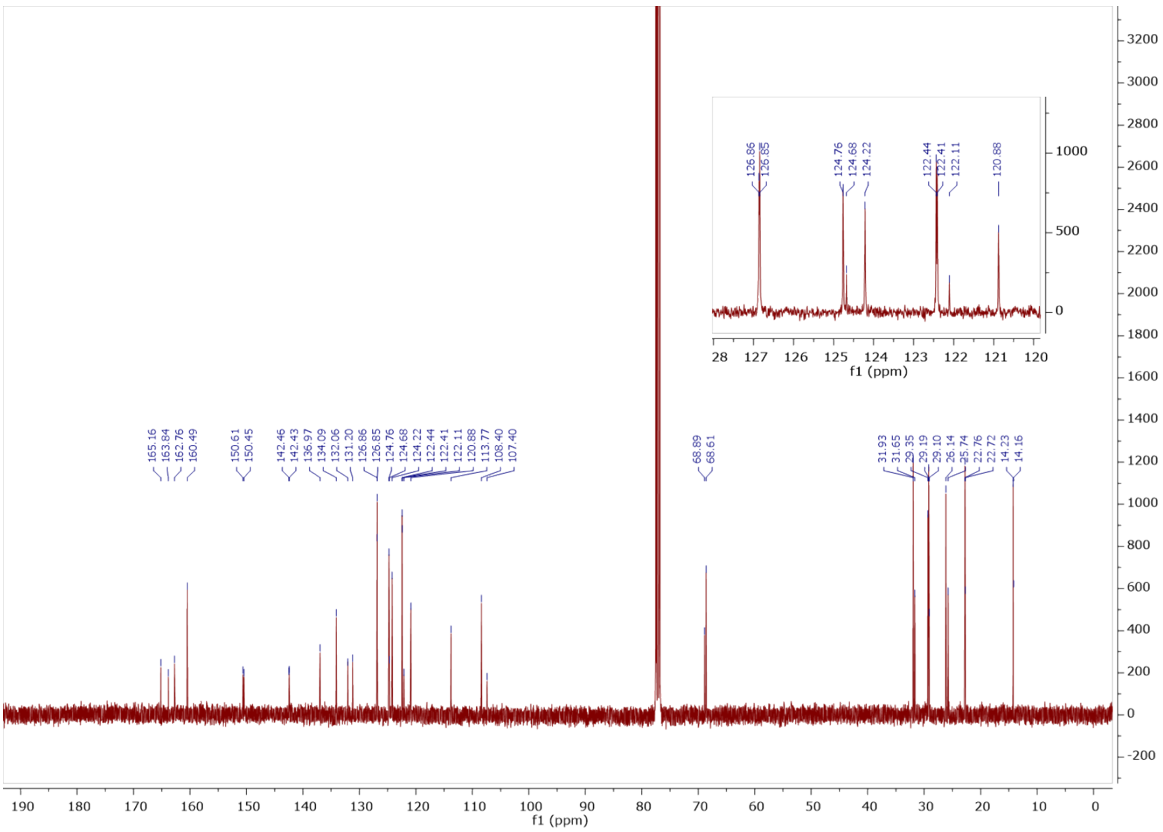

Figure S13. ^{13}C-NMR Spectrum of **AHBr** in $CDCl_3$.

3. DSC Theromgrams

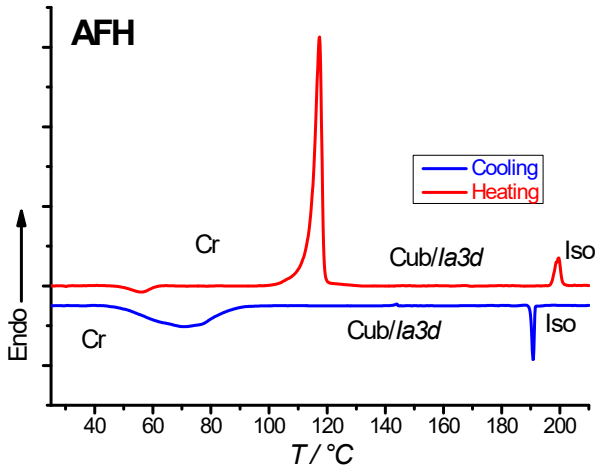

Figure S14. DSC heating and cooling traces for compound **AFH**.

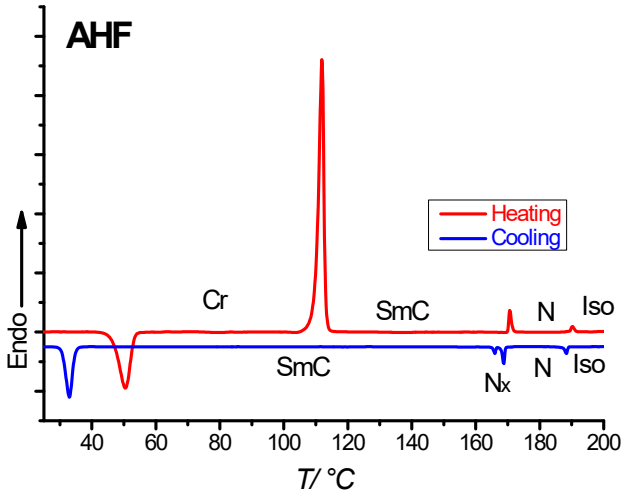

Figure S15. DSC heating and cooling traces for compound **AHF**.

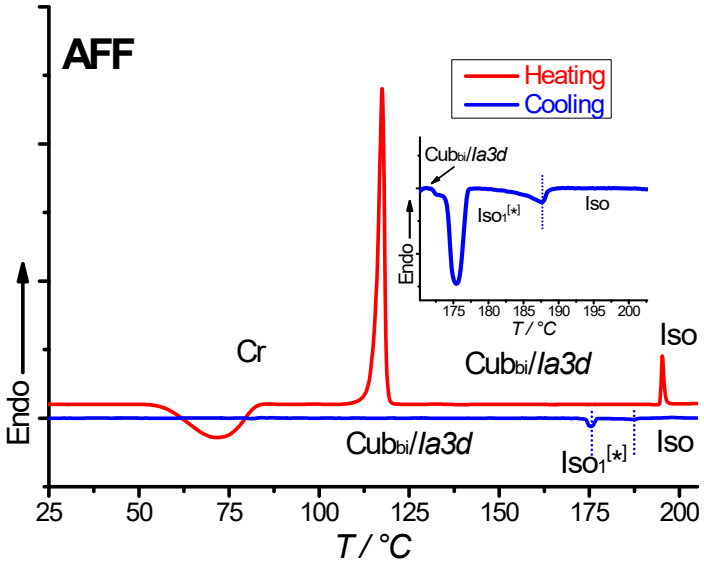

Figure S16. DSC heating and cooling traces of compound **AFF**. The inset in shows an enlarged view of the Iso-Iso$_1$[*]-Cub$_{bi}$/$Ia\bar{3}d$ transition on cooling.

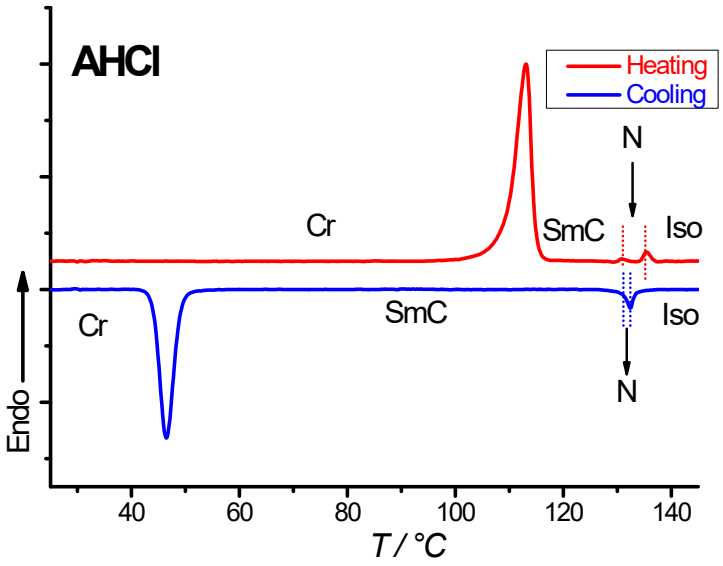

Figure S17. DSC heating and cooling traces of compound **AHCl**.

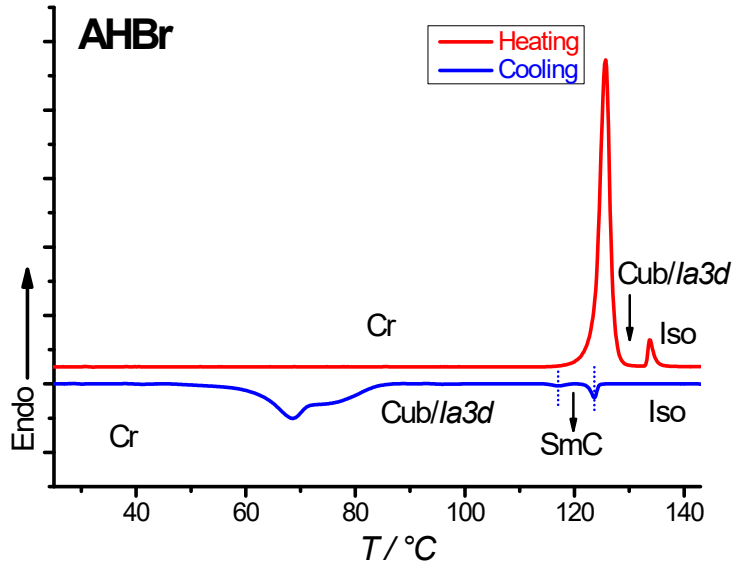

Figure S18. DSC heating and cooling traces of compound **AHBr**.

4. XRD

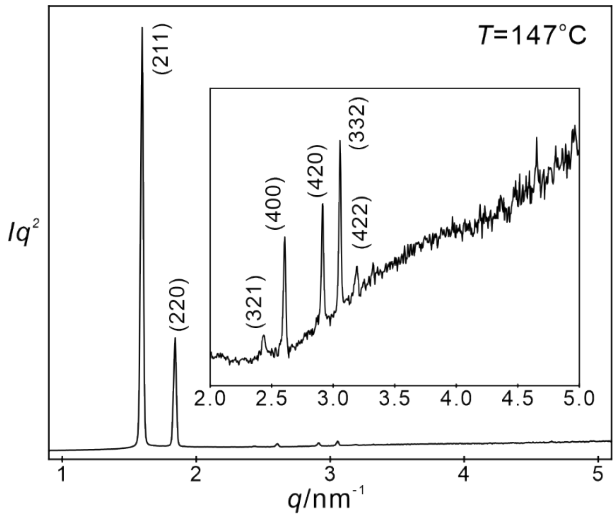

Figure S19. SAXS diffractogram of **AFF**.

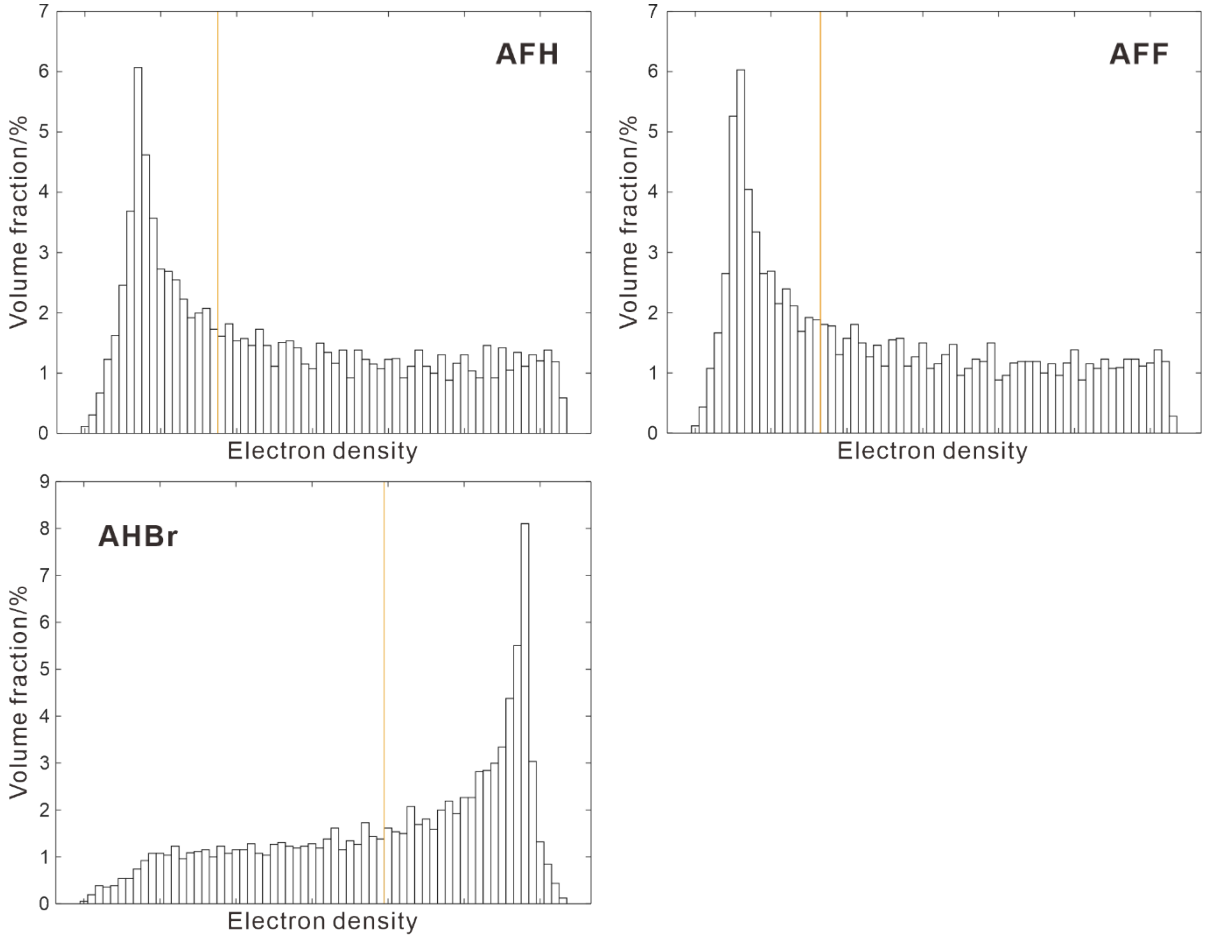

Figure S20. Electron density distribution histogram of **AFH**, **AFF** and **AHBr**.

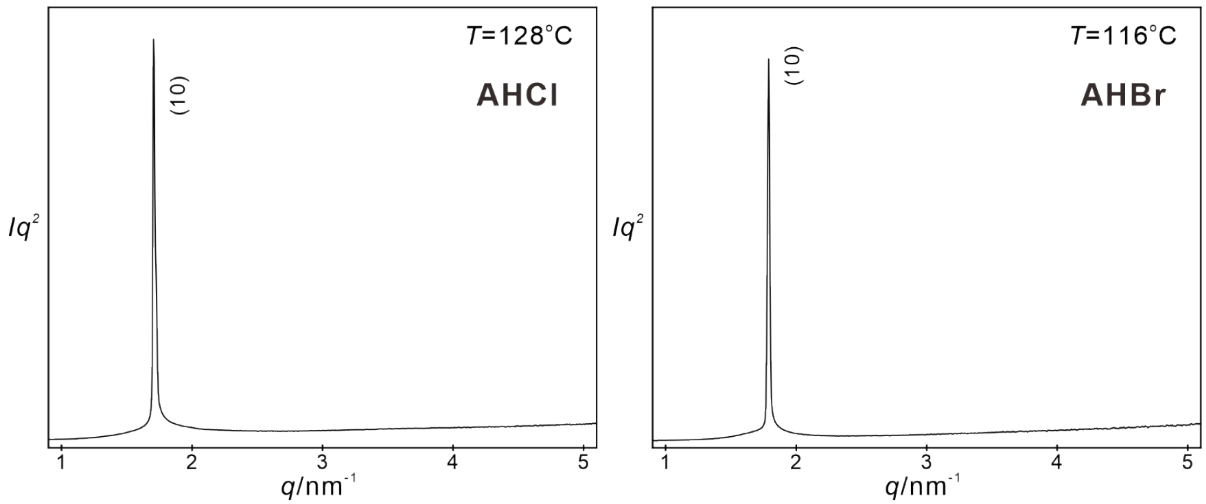

Figure S21. SAXS diffractograms of **AHCl** and **AHBr**.

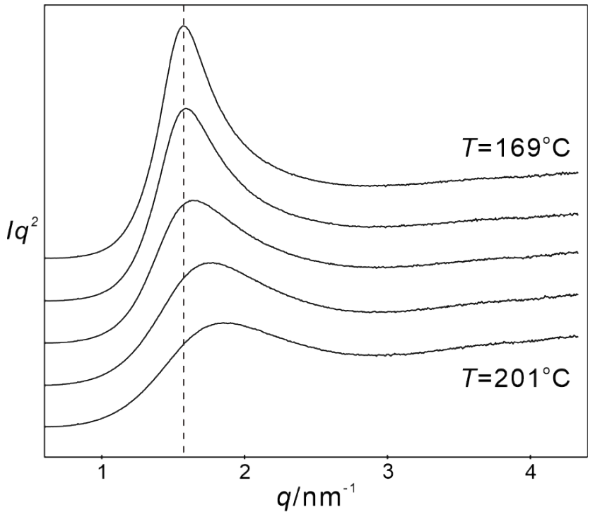

Figure S22. Temperature scan of **AHF** upon heating.

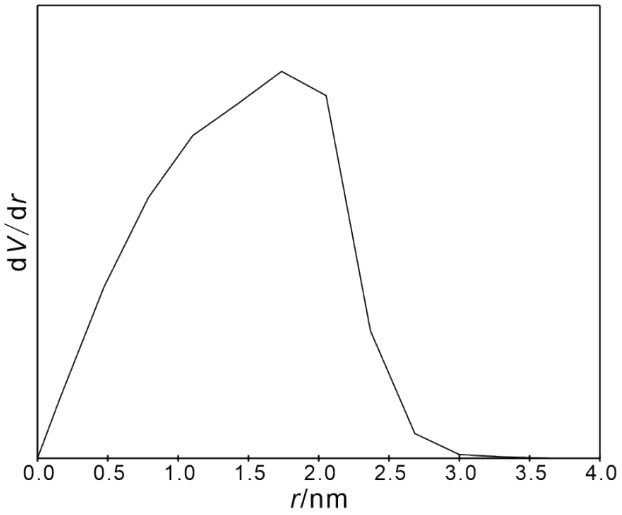

Figure S23. dV/dr curve of Cub_{bi}/$Ia\bar{3}d$ phase of **AHBr**.

Table S1 Experimental and calculated *d*-spacing of the observed SAXS reflection of the $Cub_{bi}/Ia\bar{3}d$ phase of **AFH** at 128 ºC. All intensity values are Lorentz and multiplicity corrected.

(*hkl*)	$d_{obs.}$ –spacing (nm)	$d_{cal.}$ –spacing (nm)	*intensity*	*phase*
(211)	3.98	3.98	100.0	π
(220)	3.45	3.45	53.6	π
(321)	2.61	2.61	0.2	0
(400)	2.44	2.44	3.6	0
(420)	2.18	2.18	1.3	0
(332)	2.08	2.08	1.6	0
(422)	1.99	1.99	0.3	/
(510)	1.91	1.91	0.03	/
(440)	1.72	1.72	0.2	/
(611)	1.58	1.58	0.06	/
a = 9.75 nm				

Table S2 Experimental and calculated *d*-spacing of the observed SAXS reflection of the SmC phase of **AHF** at 128 ºC. All intensity values are Lorentz and multiplicity corrected.

(*hk*)	$d_{obs.}$ –spacing (nm)	$d_{cal.}$ –spacing (nm)	*intensity*	*phase*
(10)	3.84	3.84	100.0	π
d = 3.84 nm				

Table S3 Experimental and calculated *d*-spacing of the observed SAXS reflection of the $Cub_{bi}/Ia\bar{3}d$ phase of **AFF** at 147 ºC. All intensity values are Lorentz and multiplicity corrected.

(*hk*)	$d_{obs.}$ –spacing (nm)	$d_{cal.}$ –spacing (nm)	*intensity*	*phase*
(211)	3.94	3.94	100.0	π
(220)	3.41	3.42	53.7	π
(321)	2.58	2.58	0.1	0
(400)	2.41	2.41	2.7	0
(420)	2.16	2.16	0.7	0
(332)	2.06	2.06	0.9	0
(422)	1.97	1.97	0.2	/
a = 9.66 nm				

Table S4 Experimental and calculated *d*-spacing of the observed SAXS reflection of the SmC phase of **AHCl** at 128 ºC. All intensity values are Lorentz and multiplicity corrected.

(*hk*)	$d_{obs.}$ –spacing (nm)	$d_{cal.}$ –spacing (nm)	*intensity*	*phase*
(10)	3.68	3.68	100.0	π
d = 3.68 nm				

Table S5 Experimental and calculated *d*-spacing of the observed SAXS reflection of the $Cub_{bi}/Ia\bar{3}d$ phase of **AHBr** at 125 ºC. All intensity values are Lorentz and multiplicity corrected.

(*hk*)	$d_{obs.}$ –spacing (nm)	$d_{cal.}$ –spacing (nm)	*intensity*	*phase*
(211)	3.75	3.75	100.0	0
(220)	3.25	3.25	51.1	0
(321)	2.46	2.46	0.1	0
(400)	2.30	2.30	2.2	π
(420)	2.06	2.05	0.5	π
(332)	1.96	1.96	1.9	π
(422)	1.88	1.88	0.3	/
(431)/(510)	1.80	1.80	0.2/0.4	/
a = 9.19 nm				

Table S6 Experimental and calculated *d*-spacing of the observed SAXS reflection of the SmC phase of **AHBr** at 116 ºC. All intensity values are Lorentz and multiplicity corrected.

(*hk*)	$d_{obs.}$ –spacing (nm)	$d_{cal.}$ –spacing (nm)	*intensity*	*phase*
(10)	3.51	3.51	100.0	π
d = 3.51 nm				

Table S7 Structural information of $Cub_{bi}/Ia\bar{3}d$ phase of **AFH** and **AFF**.

(*hk*)	a_{cub}/nm	n_{cell} [a]	L_{seg}/nm [b]	Φ/º [c]	n_{raft} [d]
AFH	9.75	617	3.45	9.19	3.35
AFF	9.64	584	3.41	9.30	3.21

[a] Number of molecules per cell (n_{cell}) is calculated by assuming the density of all compounds as 1g/cm^3.
[b] Length of segment between neighboring three-way junctions (L_{seg}) is calculated as $0.354a_{cub}$.
[c] Twisting angle of neighboring rafts (Φ) is calculated as $70.5/(L_{seg}/0.45)$.
[d] Number of molecules per raft (n_{raft}) is calculated as $n_{cell}/24/(L_{seg}/0.45)$.

5. Fluorescence spectroscopy

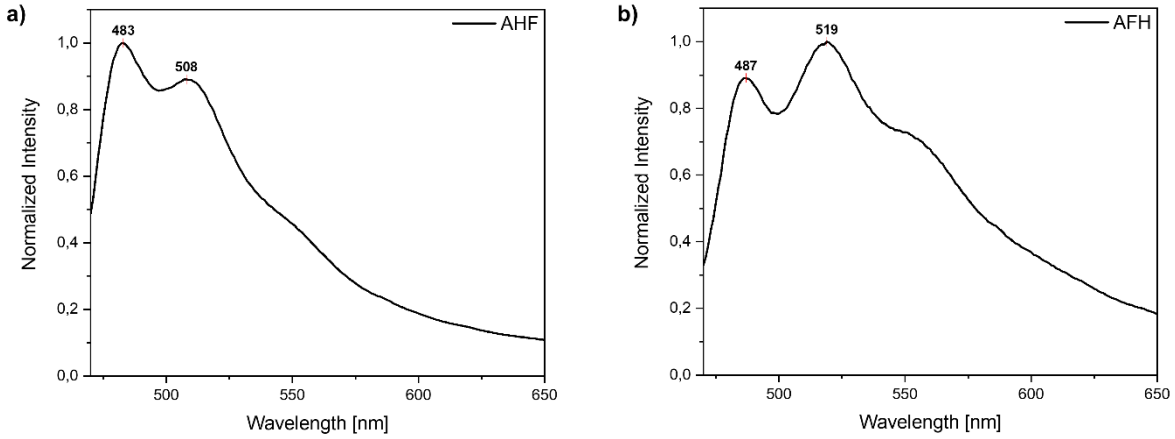

Figure S24. Normalized Emission spectra of solid-state emission of **AHF** (a, excitation wavelength 450 nm) and **AFH** (b, excitation wavelength 455 nm) at room temperature.

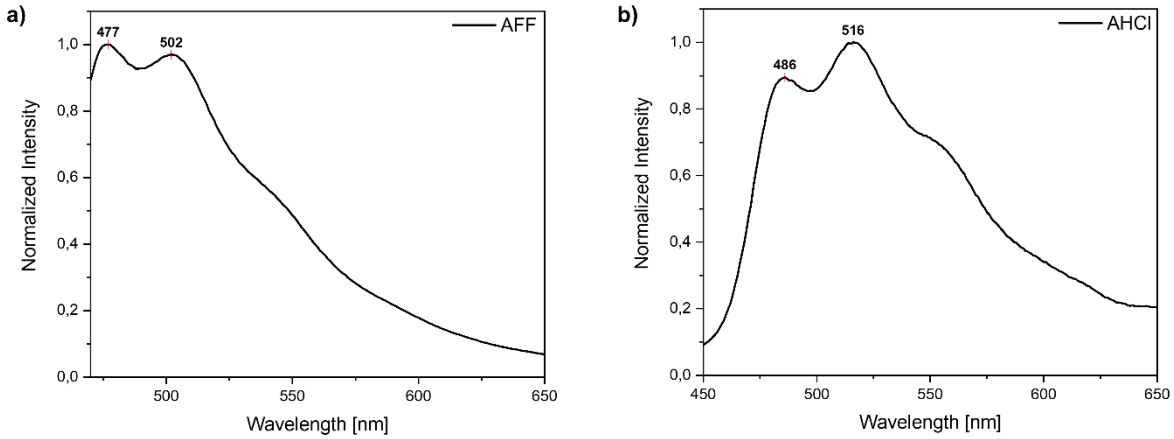

Figure S25. Normalized Emission spectra of solid-state emission of **AFF** (a, excitation wavelength 450 nm) and **AHCl** (b, excitation wavelength 450 nm) at room temperature.

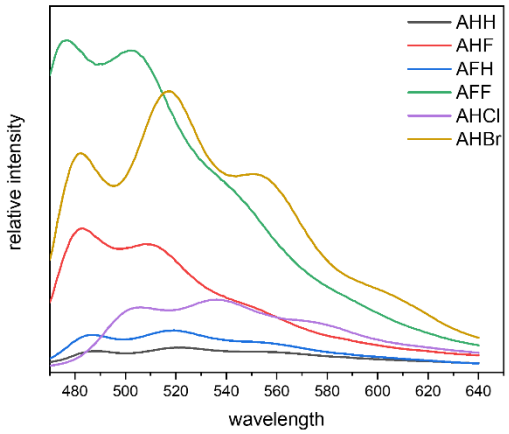

Figure S26. Relative Emission spectra of solid-state emission at room temperature of all polycatenars with ideal excitation wavelengths respectively.

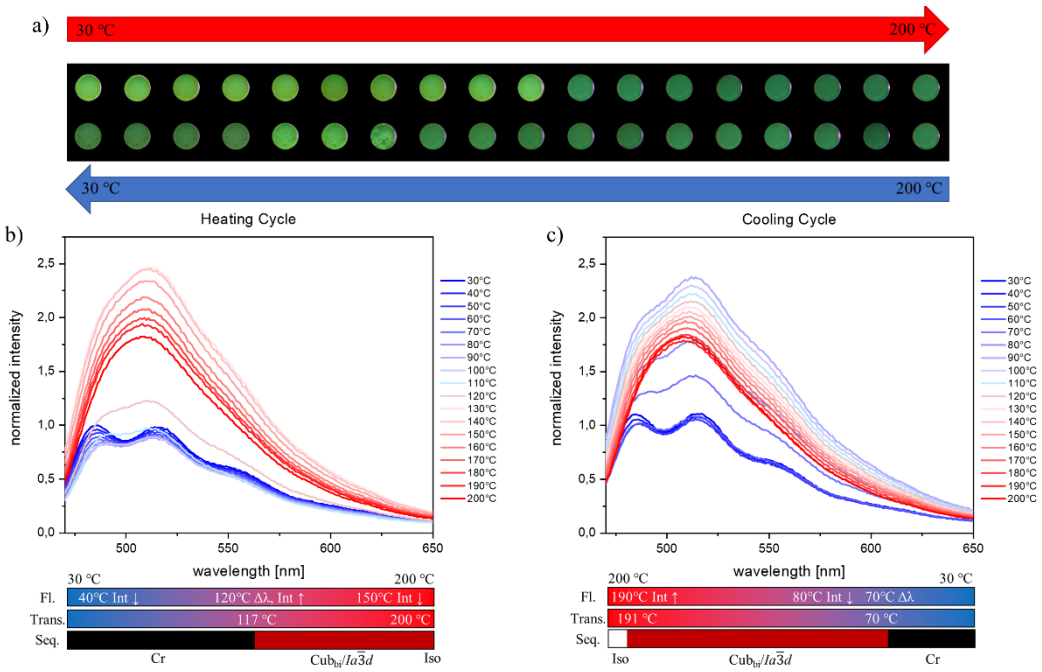

Figure S27. a) Photographs of **AFH** during heating and cooling under UV-light (395 nm). Pictures were taken every 10 °C for the heating and cooling cycle respectively. b) Normalized Emission spectra of **AFH** (excitation wavelength 450 nm) during the heating cycle. Starting with 30 °C data was collected every 10°C until reaching 200 °C. c) Normalized Emission spectra of **AFH** (excitation wavelength 450 nm) during the cooling cycle. Starting with 200 °C data was collected every 10 °C until reaching 30 °C.

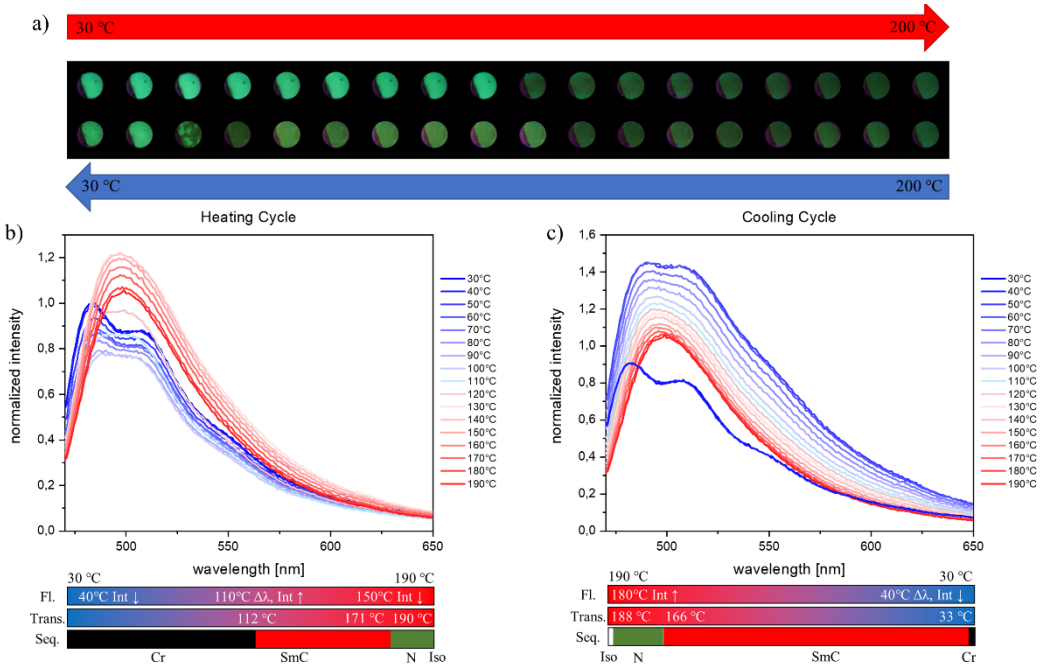

Figure S28. a) Photographs of **AHF** during heating and cooling under UV-light (395 nm). Pictures were taken every 10 °C for the heating and cooling cycle respectively. b) Normalized Emission spectra of **AHF** (excitation wavelength 450 nm) during the heating cycle. Starting with 30 °C data was collected every 10°C until reaching 190 °C. c) Normalized Emission spectra of **AHF** (excitation wavelength 450 nm) during the cooling cycle. Starting with 190 °C data was collected every 10 °C until reaching 30 °C.

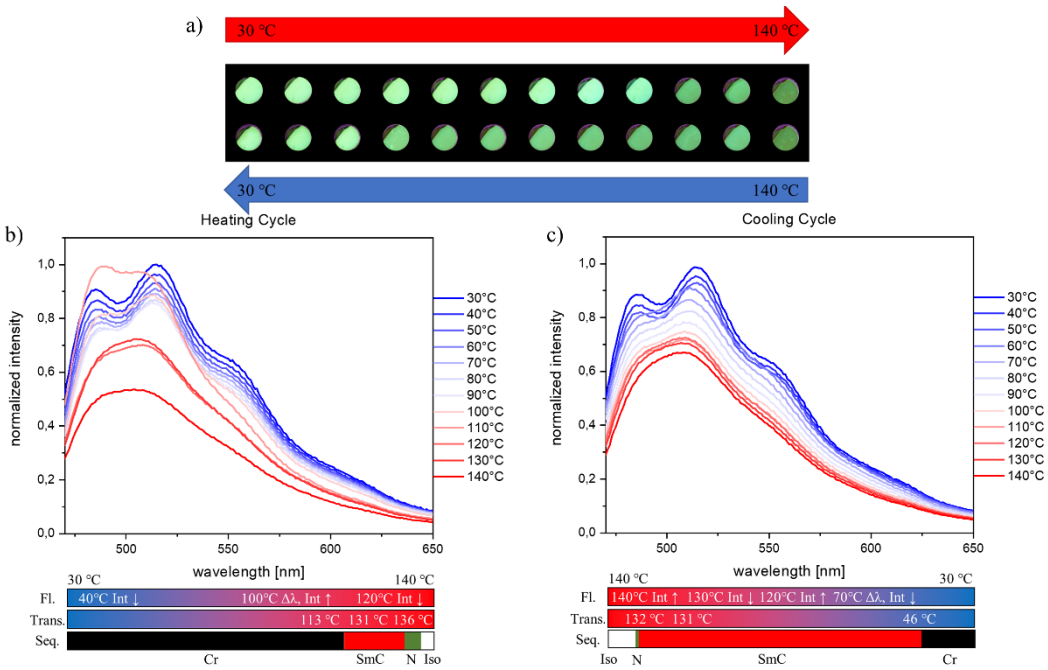

Figure S29. a) Photographs of **AHCl** during heating and cooling under UV-light (395 nm). Pictures were taken every 10 °C for the heating and cooling cycle respectively. b) Normalized Emission spectra of **AHCl** (excitation wavelength 450 nm) during the heating cycle. Starting with 30 °C data was collected every 10°C until reaching 140 °C. c) Normalized Emission spectra of **AHCl** (excitation wavelength 450 nm) during the cooling cycle. Starting with 140 °C data was collected every 10 °C until reaching 30 °C.

6. References

1. T. Reppe, S. Poppe and C. Tschierske, *Chem. Eur. J.* 2020, **26**, 16066.

2. M. Alaasar, A. F. Darweesh, C. Anders, K. Iakoubovskii and M. Yoshio, *Mater. Adv.* 2024, **5**, 561.